

# Seismic Safety of Buildings vs Other Risks in Italy: Preliminary Analysis

Adriana Pacifico

*Dipartimento di Strutture per l'Ingegneria e l'Architettura, Università degli Studi di Napoli Federico I, Italy. E-mail: adriana.pacifico@unina.it*

Iunio Iervolino

*Dipartimento di Strutture per l'Ingegneria e l'Architettura, Università degli Studi di Napoli Federico I, Italy. E-mail: iunio.iervolino@unina.it*

Performance-based earthquake engineering, typically, computes the rate of seismic events causing structural failure as a measure of seismic risk. The 2015-2017 Italian research program, *Rischio Implicito – Norme Tecniche per le Costruzioni*, has evaluated the failure rates of some code-conforming buildings varying in structural typology and configuration, designed ad-hoc for three Italian sites characterized by low, mid and high seismic hazard levels.

In the modern practice of decision analysis, the concept of micromort, defined as one-in-a-million chance of death, is used to compare different sources of risk people are subject to. The goal of this study is to compare the annual fatality rates, due to the seismic failure of code-conforming Italian structures, with micromorts (per year) associated with different causes in Italy. To obtain these micromorts/year, data from the Italian national statistical institute are analyzed. Results, although very preliminary and subjected to the working assumptions, seems to indicate that the probability of death due to an earthquake event is lower than the one due to the other analyzed causes of death, especially for comparatively low seismicity sites.

*Keywords:* seismic risk, micromort, failure rate, fatality risk, code-conforming structures reliability.

## 1. Introduction

The rate of the seismic events causing structural failure,  $\lambda_f$ , is commonly used as an index of seismic risk. It is defined as the expected number of the seismic events that, in one year, cause the reaching or the exceeding of a certain damage state. It summarizes both information about the seismic fragility of the structure and the hazard of the construction site.

A large research program in Italy, *Rischio Implicito – Norme Tecniche per le Costruzioni* or RINTC (RINTC-Workgroup, 2018) has evaluated the failure rates of several code-conforming buildings located in Italian sites characterized by different levels of seismicity. The scope of this work is to compare the fatality risk due to the structural failure of the code-conforming Italian structures studied in RINTC project, and the probability of death associated with different causes in the country. To this end, this study calculates the so-called fatality rate,  $\lambda_d$ , for the RINTC buildings, using the approach of HAZUS (FEMA, 2004).

To evaluate the probability of dying because of diseases or fatal accidents in Italy, the concept of micromort, mM, (Howard 1980) is adopted. In fact, a micromort is defined as one-in-a-million chance of death and it is commonly used in order to compare the risks associated to various events, such as specific surgery or medical treatments or some recreational activities, people are subject or

take part to. To compute mM for fatalities due to some common causes, recent data from the Italian national statistical institute are used.

The paper is structured such that, the next two sections describe RINTC project and the evaluation method for the failure rates. Subsequently, fatality rates are presented and the methodology for their evaluation is described. Then the micromorts related to some risks in Italy are computed and compared to the seismic fatality rates. Final remarks close the paper.

## 2. The RINTC Project

Within the RINTC project (RINTC-Workgroup., 2018), a set of buildings according to the Italian currently-enforced building code (CS.LL.PP., 2008, 2018), were designed, modelled and analyzed. The considered buildings vary in material/typology (i.e., reinforced concrete or RC, steel or STEEL, precast reinforced concrete or PRC, unreinforced masonry structures or URM and base-isolated reinforced-concrete buildings or BI) and configuration (e.g., with or without infillings), so as to represent as much as possible residential and industrial standard modern Italian constructions. Furthermore, structures were designed for three Italian sites characterized by low, mid and high design seismic hazard levels (Milan, Naples and L'Aquila respectively) and for different soil condition (soil A and soil C according to Eurocode 8; CEN, 2003).

In the project, seismic structural safety was quantified via the failure rate,  $\lambda_f$ , that is defined as the expected number of the seismic events that, in one year, cause structural failure; i.e., some undesired performance. In particular, for each structure two failure rates were evaluated considering two performance levels, or damage states, DS: (i) *Usability-Preventing Damage* or UPD and (ii) *Global Collapse* or GC (see Iervolino et al., 2018, for details).

Failure rates were evaluated integrating the probability of structural failure given a certain value of a ground motion intensity measure or IM,  $P[F|IM=x]$ , that is, the *fragility* of the structure, and the absolute value of the derivative – multiplied by  $d(im)$  – of the *hazard curve*, computed via probabilistic seismic hazard analysis or PSHA (Mc Guire, 2004), at the site where the structure is located. The hazard curve, for a ground motion intensity measure (IM), provides the annual rate,  $\lambda_{IM}$ , of exceedance of all possible IM values. The equation for the integration is:

$$\lambda_f = \int_x P[F|IM=x] \cdot |d\lambda_{IM}(x)|. \quad (1)$$

To obtain the seismic fragility of the considered buildings, *multi-stripe* nonlinear dynamic analyses or MSA (Jalayer, 2003) were performed at ten IM values corresponding to ten exceedance return periods of the considered ground motion intensity measure from  $10^1$  to  $10^5$  years. The chosen IM is the spectral acceleration at a period close to the fundamental vibration periods of each structure. According to the *conditional spectrum method* (Lin et al. 2013), for each IM level, twenty records were selected as an input for the MSA of nonlinear three-dimensional structural models of the buildings.

The fragility, that is, the probability of structural failure at each of the ten considered IM levels was evaluated as:

$$P[F|IM=x] = \left\{ 1 - \Phi \left[ \frac{\log(edp_f - \mu_{\log(EDP|IM=x)})}{\sigma_{\log(EDP|IM=x)}} \right] \right\} \times \left( 1 - \frac{N_{col,IM=x}}{N_{tot,IM=x}} \right) + \frac{N_{col,IM=x}}{N_{tot,IM=x}} \quad (2)$$

In the equation,  $edp_f$  is a value of an engineering demand parameter (EDP) defining the limit that, if passed, determines the DS of interest;  $\Phi(\bullet)$  denotes the cumulative Gaussian distribution function and  $\mu_{\log(EDP|IM=x)}$ ,  $\sigma_{\log(EDP|IM=x)}$  are the mean and the standard deviation of the logarithms of EDP given IM, respectively. These parameters are estimated

using the results of the analyses yielding meaningful EDP values. However, for some analysis the EDP is not available, because of *global instability*, according to the terminology of Shome and Cornell (2000), can occur. These cases are usually referred to as *collapse cases* and  $N_{col,IM=x}$  indicates their number at the considered IM stripe, while  $N_{tot,IM=x}$  is the total number of performed nonlinear dynamic analyses at the same stripe.

An example of the results of MSA, for one of the studied URM structure, for which the IM is the spectral acceleration at 0.15s or  $Sa(T=0.15s)$ , is reported in Fig. 1; scatters represent the results of single nonlinear dynamic analyses.

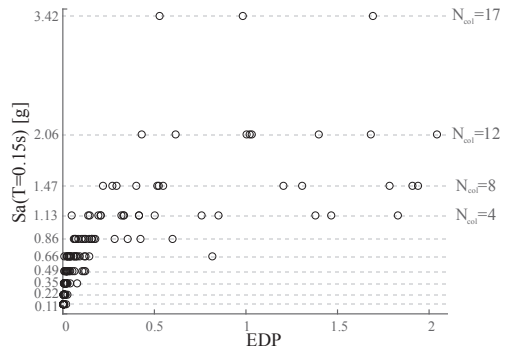


Fig. 1 Example of MSA result for a structural from the RINTC project.

Before proceeding any further, to avoid some possible confusion, it must be clarified that the word *collapse* is used with three different meanings through this paper. The first one is the one mentioned in the previous section, when talking about GC, which is one performance level from the RINTC project. The second one is the global instability in the fragility evaluation just mentioned. Finally, collapse as it is intended in section 4 to compute the fatality rates.

### 3. Failure rates as computed in this study

In this study, STEEL, PRC and a part of RC and URM buildings are considered.

STEEL structures from the RINTC project are one story rectangular industrial buildings featuring moment resisting frames in the transverse direction and concentrically braced frames in the longitudinal direction. Four different configurations (denoted as Geo1-4) are considered varying, transverse and longitudinal bay widths and the story height (Scozzese et al., 2018).

PRC structures also are single-story industrial buildings that have precast columns fixed at the base and connected at the top to longitudinal precast prestressed beams through dowel connections. The girder beams are connected to the column forks. Vertical precast panels are the cladding system. Four different configurations (denoted as Geo1-4) are considered varying transverse and longitudinal bay widths and the story height (Magliulo et al., 2018).

As it regards RC structures, three-, six-, and nine-story (3st, 6st, 9st) RC moment resisting frame buildings, bare and infilled, were studied (Ricci et al., 2018). Only those with the infill configurations (i.e., infilled-frames, IF, and pilotis-frames, PF) were considered in this work.

Among the URM structures designed in RINTC project, the two- and three-story (2st, 3st) URM buildings made of perforated clay units with mortar joints, denoted as C-type and I-type were considered. They present different architectural configurations (Manzini et al., 2018; Cattari et al., 2018).

Table 1 summarizes the analyzed structures for each site and each soil condition. For these structures, failure rates were computed again for the purposes of this study, departing from the RINTC procedure. In fact, Eq. (1) was used, but some differences (discussed in the next section) in the evaluation of the fragility of the structures were adopted.

Table 1. Analyzed structures.

Site	URM	RC	STEEL	PRC
L'Aquila Soil A	(2,3)st_C1, 2st_C3, 2st_I1.	9st_PF, 9st_IF.	Geo1-4	Geo1-4
L'Aquila Soil C	2st_C3, 2st_I1.	(3,6,9)st_PF, (3,6,9)st_IF.	Geo1-4	Geo1-4
Naples Soil A	(2,3)st_C1, 2st_C3, 3st_C4, 3st_I2, 2st_C1, 2st_C2,	-	Geo1-4	Geo1-4
Naples Soil C	2st_C4, 2st_I1, 3st_C3, 3st_C5, 3st_I2.	(3,6,9)st_PF, (3,6,9)st_IF.	Geo1-4	Geo1-4
Milan Soil A	2st_C1, 2st_C4, 3st_C2, 3st_C6.	-	Geo1-4	Geo1-4
Milan Soil C	2st_C1, 2st_C7, 3st_C2.	(3,6,9)st_PF, (3,6,9)st_IF.	Geo1-4	Geo1-4

### 3.1 Fragility functions

In the RINTC project, structural fragility was evaluated only referring to the ten IM levels of the MSA. Herein, in order to account for the probability of failure conditional to the occurrence of any value of IM, a lognormal fragility function, Eq. (3), is chosen:

$$P[F|IM = x] = \Phi \left[ \frac{\ln(x) - \mu}{\sigma} \right]. \quad (3)$$

The parameters of the fragility model,  $\{\mu, \sigma\}$ , were obtained for each structural model via the R2R-EU software (Baraschino et al., 2020) considering the results of non-linear dynamic analysis from the RINTC project. As an example, in Fig. 2 some fragilities of the type in Eq. (3) (solid curves) obtained are compared with the results (scatters) of Eq. (2).

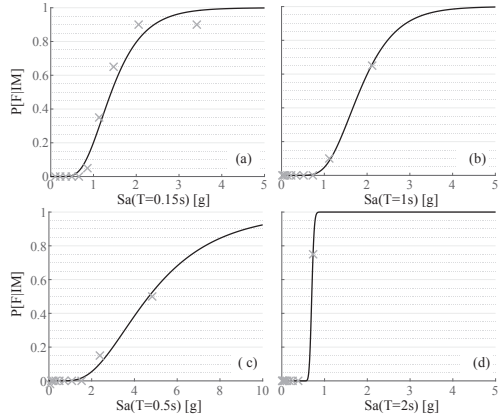


Fig. 2 Example of lognormal cumulative distribution function used to fit fragility function of a URM (a), RC (b), STEEL (c) and PRC (d) RINTC structure.

### 3.2 Hazard curves

Hazard curves for the considered IMs at the three sites were evaluated via classical PSHA, using the REASSES software (Chioccarelli et al., 2019) considering the input data of the branch 921 of the logic tree that was used to build the official Italian hazard map (Stucchi et al., 2011) and using the Ambrasey et al. (1996) ground motion prediction equation.

To be consistent with the IMs used for fragility assessment, hazard curves were computed in terms of pseudo-acceleration spectral ordinates at the periods  $T = \{0.15s, 0.50s, 1.00s, 1.50s, 2.00s\}$  that represent the first-mode vibration periods of RINTC buildings. Fig. 3 shows the hazard curves for L'Aquila, Naples and Milan expressed in terms peak ground acceleration (PGA) to compare the different hazard of the sites.

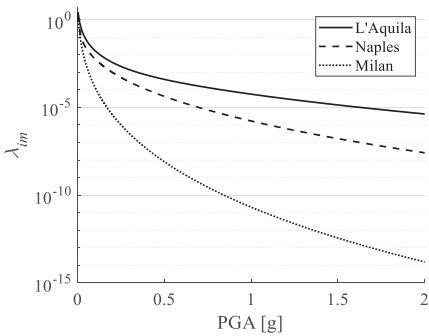


Fig. 3 Example of hazard curves for the three considered sites for Soil A.

### 3.3 Failure rates

The failure rates of the considered typologies are presented in this section (i.e., Table 1). They are simply the arithmetic averages taken across the failure rates of the analyzed buildings of a given typology.

For representation purposes, the failure rates were grouped per structural typology (URM, RC, STEEL and PRC). In particular, results are given in Fig. 4 and Table 2 and in Fig. 5 and Table 3 for GC and UPD, respectively. Failure rates values lower than 1E-05 were set to 1E-05; see Iervolino et al. (2018) for a discussion on this issue.

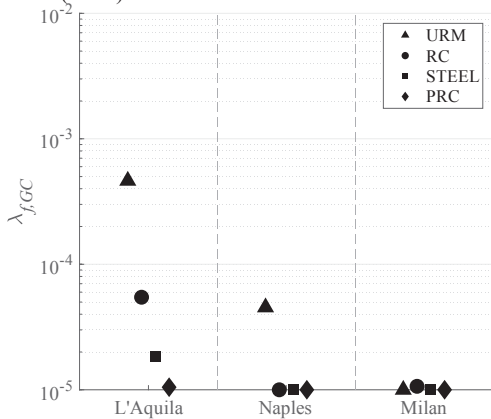


Fig. 4 Failure rates for CG damage state.

In the figures, the marks represent, one for each typology, the values of the evaluated  $\lambda_f$ . One can see from the figures that the rates tend to decrease with the decreasing hazard for the site (see also Fig. 3), which was one of the main results of the RINTC project.

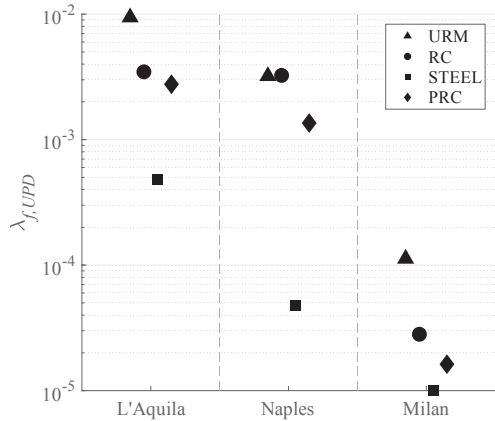


Fig. 5 Failure rates for UPD damage state.

Table 2. Failure rates for GC damage state.

Structural typology	L'Aquila	Naples	Milan
URM	4.63E-04	4.52E-05	1.00E-05
RC	5.46E-05	1.00E-05	1.06E-05
STEEL	1.83E-05	1.00E-05	1.00E-05
PRC	1.05E-05	1.00E-05	1.00E-05

Table 3. Failure rates for UPD damage state.

Structural typology	L'Aquila	Naples	Milan
URM	9.43E-03	3.21E-03	1.12E-04
RC	3.47E-03	3.25E-03	2.81E-05
STEEL	4.83E-04	4.81E-05	1.00E-05
PRC	2.76E-03	1.35E-03	1.62E-05

## 4. Fatality Rate

The earthquake fatality rate,  $\lambda_d$ , can be seen as the product of the probability of dying given the occurrence of the seismic event,  $P[D|E]$ , and the rate of earthquake occurrence,  $\nu$  at the construction site. Thus, according to the total probability theorem, it is possible to evaluate  $\lambda_d$  following Eq. (4):

$$\lambda_d = \nu \cdot P[D|E] = \nu \cdot \sum_{i=1}^n P[D|DS_i] \cdot P[DS_i|E] \quad (4)$$

in which  $n$  is the number of the considered damage states,  $P[D|DS_i]$  is the probability of death given the reaching of the  $i$ -th damage state and  $P[DS_i|E]$  is the probability that the structure reaches the  $i$ -th damage state given the earthquake occurrence. The latter has to be evaluated as the difference of the probability to reach or exceeding the  $i$ -th damage state and the probability to reach

or exceeding the  $(i+1)$ -th damage state, as it is shown in Eq (5):

$$P[DS_i|E] = P[DS \geq DS_i|E] - P[DS \geq DS_{i+1}|E] \quad (5)$$

Based on the total probability theorem,  $P[DS \geq DS_i|E]$  can be computed as:

$$P[DS \geq DS_i|E] = \int_0^{+\infty} P[F_{DS_i}|IM=x] \cdot f_{IM|E}(x) dx = \int_x P[F_{DS_i}|IM=x] \cdot d\lambda_{IM}(x) \quad (6)$$

where  $P[F_{DS_i}|IM=x]$  is the probability to reach or exceed the  $i$ -th damage state given a certain IM value, that is, the fragility function referring to the  $i$ -th damage state, and  $f_{IM|E}$  is the probability density function of the IM, conditional to the earthquake event occurrence. This means that, multiplying  $P[DS \geq DS_i|E]$  by the earthquake rate yields the failure rate:

$$v \cdot P[DS \geq DS_i|E] = \lambda_{f,DS_i} \quad (7)$$

In particular, for the application of this work, Eq. (4) becomes Eq. (8):

$$\lambda_d = P[D|UPD] \cdot (\lambda_{f,UPD} - \lambda_{f,GC}) + P[D|GC] \cdot \lambda_{f,GC} \quad (8)$$

In this study, preliminarily,  $P[D|DS]$  is evaluated from the fatality rates given the structural failure,  $\lambda_{d|DS}$ , which were obtained from HAZUS. In particular, it was assumed  $P[D|DS] = \lambda_{d|DS}$ .

In fact, the use of the HAZUS approach requires further considerations.  $P[D|GC]$  is computed considering that GC corresponds to *complete structural damage* (CSD), see Tsang & Wenzel (2016), and the probability of death is conditional on structural collapse is computed as:

$$P[D|GC] = P[D|GC,indoor] \times P[indoor|GC] + P[D|GC,outdoor] \times \{1 - P[indoor|GC]\} \quad (9)$$

Where the probability of being indoor at the time of failure,  $P[indoor|GC]$ , is assumed to be equal to 0.9. The probability of death given being indoor in the building is computed further splitting in the fact that GC leads to *collapse* or not:

$$P[D|GC,indoor] = P[D|GC,indoor,collapse] \times P[collapse|GC] + P[D|GC,indoor,nocollapse] \times \{1 - P[collapse|GC]\} \quad (10)$$

where  $P[collapse|GC]$  is taken from HAZUS as well, assuming that it coincides with CSD. Also the probability of dying being *outdoor*,  $P[D|GC,outdoor]$ , it taken from HAZUS.

Finally, HAZUS provides fatality rates considering different *injury severity levels*. Herein, two were considered: (i) *severity 3: injuries that pose an immediate life-threatening condition if not treated adequately and expeditiously*; (ii) *severity 4: instantaneously killed or mortally injure*. Therefore, it is, for  $P[D|GC,indoor,collapse]$ :

$$P[D|GC,indoor,collapse] = P[severity3|GC,indoor,collapse] + P[severity4|GC,indoor,collapse] \quad (11)$$

The same applies for  $P[D|GC,nocollapse]$ .

Finally, to evaluate  $P[D|UPD]$  the same approach is applied, considering that UPD corresponds to *moderate structural damage* of HAZUS; in this case  $P[collapse|UPD] = 0$ .<sup>a</sup>

The obtained fatality rates are exposed in Table 4 and are interpreted as about equal to the annual probability of an individual continuously exposed to the structural failure of a building of a specific typology at a specific site. However, they are simply arithmetic averages of fatality rates of the buildings in Table 1, without any relative weighting of the various configurations and possible occupancies.

Table 4. Fatality rates.

Structural typology	L'Aquila	Naples	Milan
URM	1.01e-05	1.04e-06	2.17e-07
RC	9.70e-07	1.80e-07	1.92e-07
STEEL	2.04e-07	1.12e-07	1.12e-07
PRC	2.19e-07	2.09e-07	2.09e-07

## 5. Micromort

A micromort (mM) is defined as one-in-a-million chance of death. Micromorts are a tool used in the

<sup>a</sup> Zuccaro and Cacace (2011) provide the same kind of probabilities, which were used in Iervolino et al. (2015) for fatality risk evaluations.

decision analysis to compare different risks; e.g., Fryet al. (2016), Radanliev et al. (2018).

With the aim to obtain micromort/year associated with different causes of death in Italy, data form ISTAT (i.e., the Italian national institute of statistic), from 2012 to 2016, were retrieved and then normalized with the number resident population on January 1<sup>st</sup> of the relative year of analysis. In this way, the nationwide average number of the death per year is obtained. These numbers per million represent the micromorts for the different considered causes of death. The analyzed causes are:

- (IP) *infectious and parasitic diseases* (tuberculosis, HIV, viral hepatitis, others);
- (T) *tumors*;
- (NS) *diseases of the nervous system and sense organs* (Parkinson's disease, Alzheimer's disease, others);
- (CS) *diseases of the circulatory system* (ischemic heart diseases, cerebrovascular diseases, others);
- (RS) *diseases of the respiratory system* (flu, pneumonia, chronic diseases of the lower respiratory tract, others);
- (AF) *accidental falls*; (RA) *road accidents* (in which car occupants or pedestrians died).<sup>b</sup>

Table 5. Micromorts associated to some causes of death in the 2016 in Italy.

Cause	micromort (mM)
IP	211.82
T	2958.88
NS	456.59
CS	3657.99
RS	767.11
AF	63.07
RA	55.27

## 5. Results

In Fig. 6 the preliminary annual fatality rates due to the seismic failure of code-conforming Italian structures caused by a seismic event are compared with the micromort/year associated with the considered risks in Italy.

First, the figure reports the average GC failure rates (grey marks) interpreting them as fatality rates. The implicit assumption in this comparison is that death is certain given GC, while it is null

given UPD. It appears that, in this case, the values of the rates are larger than the mM for the URM structures located in high and mid hazard sites; the same happens for RC structures sited in L'Aquila. Second, fatality rates (black marks), as computed per section 4, are compared Mm's. Results show that the (averaged) fatality risk due to seismic structural failure is lower than the probability of dying due to other common diseases or common fatality accidents.

The hypothesis of this comparison is that a generic individual continuously occupies a building corresponding to a specific mark, in the very same way he's continuously exposed to the micromort the lines refer to.

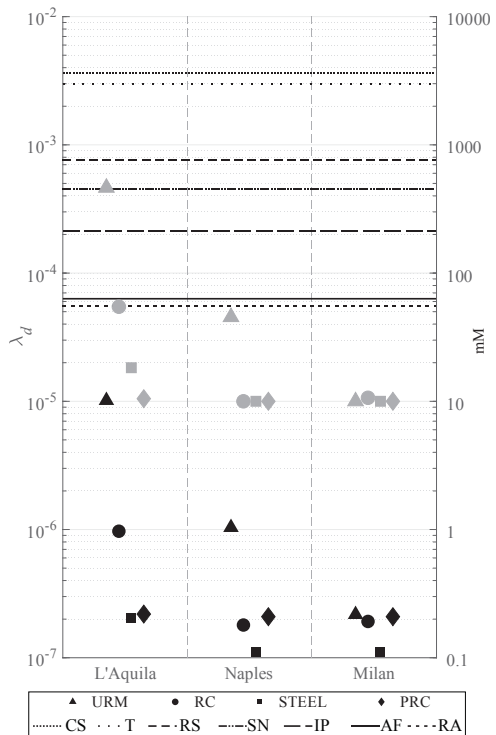


Fig. 6. annual fatality rates (black marks), failure rates associated to GC damage state (grey marks), and micromorts related to considered causes of death.

## 6. Conclusions

<sup>b</sup> The same approach can be applied at a more local scale (i.e., Milan, Naples and L'Aquila separately), but the results are similar to those presented in the table.



This study preliminarily compared the probability of dying due to the seismic structural failure of code-conforming Italian structures located in three different sites, characterized by different level of seismic hazard, and micromort/year associated with other causes of death in Italy.

The results show that, in Italy, the annual probability of dying due to some common causes seems higher than the one due to structural failure of a code-conforming building, even in the high hazard site.

### Acknowledgements

The study presented in this article was developed within the activities of the ReLUIS-DPC 2014–2018 research program, funded by *Presidenza del Consiglio dei Ministri – Dipartimento della Protezione Civile*. Opinions and conclusions do not necessarily reflect those of the funding entity. Data and technical supports from the RINTC workgroup, as well as the comments of Massimiliano Giorgio (*Università degli Studi di Napoli Federico II*), are gratefully acknowledged.

### References

- Ambraseys, N. N., Simpson, K. A., & Bommer, J. J. (1996). Prediction of horizontal response spectra in Europe. *Earthq. Eng. Struct. Dyn.*, 25(4), 371–400.
- Baraschino, R., Baltzopoulos, G., & Iervolino, I. (2020). R2R-EU: Software for fragility fitting and evaluation of estimation uncertainty in seismic risk analysis. *Soil Dyn. Earthq. Eng.*, 132, 106093.
- Cattari, S., Camilletti, D., Lagomarsino, S., Bracchi, S., Rota, M., & Penna, A. (2018). Masonry Italian Code-Conforming Buildings. Part 2: Nonlinear Modelling and Time-History Analysis. *J. Earthq. Eng.*, (accepted).
- CEN, E. C. for S. (2003). *TC250/SC8/ Eurocode 8: Design Provisions for Earthquake Resistance of Structures, Part 1.1: General rules, seismic actions and rules for buildings* (Vol. 1).
- Chioccarelli, E., Cito, P., Iervolino, I., & Giorgio, M. (2019). REASSESS V2.0: software for single- and multi-site probabilistic seismic hazard analysis. *Bull. Earthq. Eng.*, 17(4), 1769–1793.
- CS.LL.PP. (2008). *Norme tecniche per le costruzioni (in Italian)*. Gazzetta Ufficiale della Repubblica Italiana, 29, Italy.
- CS.LL.PP. (2018). Aggiornamento delle norme tecniche per le costruzioni. *Gazz. Uff. Della REPUBBLICA ITALIANA*, 42, 1–198.
- FEMA. (2004). *Multi-hazard Loss Estimation Methodology: Earthquake Model: HAZUS MR4, technical manual*.
- Fry, A. M., Harrison, A., & Daigneault, M. (2016). Short communication Micromorts - what is the risk? *Br. J. Oral Maxillofac. Surg.*, 54(2), 230–231.
- Howard, R. A. (1980). *On making life and death decisions. In Societal risk assessment: How safe is safe enough?* (J. Richard, C. Schwing, & W. A. Albers (eds.)).
- Iervolino, I., Spillatura, A., & Bazzurro, P. (2018). Seismic Reliability of Code-Conforming Italian Buildings. *J. Earthq. Eng.*, 22(sup2), 5–27.
- Jalayer, F. (2003). *Direct probabilistic seismic analysis: implementing non-linear dynamic assessments*.
- Lin, T., Haselton, C. B., & Baker, J. W. (2013). Conditional spectrum-based ground motion selection. Part I: Hazard consistency for risk-based assessments. *Earthq. Eng. Struct. Dyn.*, 42(June), 1847–1865.
- Magliulo, G., Bellotti, D., Cimmino, M., & Nascimbene, R. (2018). Modeling and Seismic Response Analysis of RC Precast Italian Code-Conforming Buildings Modeling and Seismic Response Analysis of RC Precast Italian. *J. Earthq. Eng. ISSN*, 22(2), 140–167.
- Manzini, C. F., Magenes, G., Penna, A., Rota, M., Camilletti, D., Cattari, S., Lagomarsino, S., & da Porto, F. (2018). Masonry Italian Code-Conforming Buildings: Part 1: Case Studies and Design Methods. *J. Earthq. Eng.*, (accepted).
- Mc Guire, R. K. (2004). *Seismic Hazard And Risk Analysis*. Earthq. Eng. Res. Institute, Oakland, CA.
- Radanliev, P., De Roure, D. C., Nicolescu, R., Huth, M., Montalvo, R. M., Cannady, S., & Burnap, P. (2018). Computers in Industry Future developments in cyber risk assessment for the internet of things. *Comput. Ind.*, 102, 14–22.
- Ricci, P., Manfredi, V., Noto, F., Terrenzi, M.,

- Petrone, C., Celano, F., De Risi, M. T., Camata, G., Franchin, P., Magliulo, G., Masi, A., Mollaioli, F., Spacone, E., & Verderame, G. M. (2018). Modeling and Seismic Response Analysis of Italian Code-Conforming Reinforced Concrete Buildings. *J. Earthq. Eng.*, 22(sup2), 105–139.
- RINTC-Workgroup. (2018). Results of the 2015-2018. The implicit risk of code-conforming structures in Italy. *ReLUIS Report, Rete Dei Lab. Univ. Di Ing. Sismica (ReLUIS), Naples, Italy.*
- Scozzese, F., Terracciano, G., Zona, A., Della Corte, G., Dall'Asta, A., & Landolfo, R. (2018). Modeling and Seismic Response Analysis of Italian Code-Conforming Single-Storey Steel Buildings Modeling and Seismic Response Analysis of Italian. *J. Earthq. Eng.*, 22(2), 168–197.
- Shome, N., & Cornell, C. A. (2000). Structural Seismic Demand Analysis : Consideration of “ Collapse .” *PMC2000 - 8th ASCE Spec. Conf. Probabilistic Mech. Struct. Reliab. Univ. Notre Dame, South Bend, Indiana, 24-26 July, 2000.*
- Stucchi, M., Meletti, C., Montaldo, V., Crowley, H., Calvi, G. M., & Boschi, E. (2011). Seismic Hazard Assessment ( 2003 – 2009 ) for the Italian Building Code. *Bull. Seismol. Soc. Am.*, 101(4), 1885–1911.
- Tsang, H. H., & Wenzel, F. (2016). Setting structural safety requirement for controlling earthquake mortality risk. *Saf. Sci.*, 86, 174–183.